IOP Conf. Series: Materials Science and Engineering **808** (2020) 012016 doi:10.1088/1757-899X/808/1/012016

Fibrous silica induced narrow band gap TiO_2 catalyst for enhanced visible light-driven photodegradation of methylene blue

A A Fauzi[1], A A Jalil [1,2*], M Mohamed[1], N A Naseri[1], C N C Hitam[1], N F Khusnun[1], N S Hassan[1], A F A Rahman[1], F F A Aziz[1] and M S M Azmi[3]

[1] School of Chemical and Energy Engineering, Faculty of Engineering, Universiti Teknologi Malaysia, 81310 UTM Johor Bahru, Johor, Malaysia
[2] Centre of Hydrogen Energy, Institute of Future Energy, 81310 UTM Johor Bahru, Johor, Malaysia
[3]Department of Chemistry, Faculty of Science,Universiti Teknologi Malaysia, 81310 UTM Johor Bahru, Johor, Malaysia

*aishahaj@utm.my

Abstract. Fibrous silica titania (FST) was synthesized via hydrothermal method and evaluated on photodegradation of methylene blue (MB). The catalyst was characterized using field emission scanning electron microscopy (FESEM), Fourier transform infrared (FTIR) spectroscopy, ultraviolet-visible diffuse reflectance spectroscopy (UV-Vis DRS) and N_2 adsorption–desorption. The photocatalytic activity was performed under different reaction condition namely pH, catalyst dosage and MB initial concentration. FST demonstrated higher performance (99.9%) for 10 mg L^{-1} of MB initial concentration than titania (TiO_2) using 0.25 g L^{-1} of catalyst dosage at pH 5 for 2 h. The superior performance towards photodegradation of MB under visible light demonstrated by synthesized FST was due to unique morphology of fibrous, high surface area, narrow band gap and more active site (Si-O-Ti). Kinetics study indicated that the photodegradation of MB was well fitted with pseudo-first order Langmuir-Hinshelwood model and adsorption was the rate-limiting step. The FST maintained its photocatalytic activities for up to five cycles reaction with slightly catalyst deactivation, suggesting that the FST is suitable to be implied in the photocatalytic reaction.

1. Introduction

In textile dyeing industry, 1-20% of the total world production of dyes is lost during the dyeing process [1]. Methylene blue (MB) is a cationic dye commonly used for printing, dyeing cotton, wool, and leather. Consequently, the discharged MB in wastewater can threat to aquatic life and human being due to its carcinogenic and toxicity [2]. Various alternatives have been introduced such as adsorption, biodegradation and coagulation. However, these methods have proven to be markedly ineffective due to the production of secondary pollutant, which requires high cost and energy consumption [3]. Thus, another alternatives method is urgently needed.

Advanced Oxidation Processes (AOPs) have attracted much attention among researchers for degradation of targeted pollutants due to the simple and low-cost processes [4]. Among AOPs, heterogeneous photocatalysis using semiconductors such as zinc oxide, titanium dioxide, copper oxide

and zirconium dioxide has been proved efficient for degrading aquatic and atmospheric organic contaminants through the hydroxyl radicals. Among semiconductor photocatalysts, titanium dioxide (TiO_2) is widely used in various areas such as photocatalysis, self-cleaning and dye-sensitized solar cells due to its excellent chemical and physical properties, strong photooxidation power and low cost [4]. However, TiO_2 consists of several shortcomings including low surface area, wide band gap, less electron hole separation and difficulty in isolation and reusability [6,7], which reduce its performance for adsorption and degradation of pollutant in visible light. Hence, the modification of TiO_2 is required in order to improve the performance in visible light.

To overcome these drawbacks, most of researchers have interested on coupling of TiO_2 with porous silica in order to prevent the agglomeration of TiO_2 particles and increase surface area [8]. Previous studies have been reported the synthesis of nanostructured TiO_2 or TiO_2 supported on this supports can enhance surface area and particle size [6]. Moreover, it has been found that the coupling of SiO_2 with TiO_2 able to effectively prevent charge recombination in dye-sensitized solar cell [8]. The synthesis of Ti-containing large pores materials such as mesoporous silica (MS) has been also reported [9]. In spite of this modification enhance the properties of TiO_2 supported on porous material, the accessibility of pollutant towards catalyst seemed decreasing due to tubular structure and high possibility of pores clogging which partially collapse after thermal treatment.

Latterly, fibrous morphology has aroused attention among researches in enhancing the performance due to its unique morphology, high accessibility of active sites and surface area [10]. In addition, this morphology has open pore channels and controllable pore sizes during synthesis such as by altered amount of surfactant, heating and stirring time. Besides, morphological modification of the catalysts also was extensively developed aiming the active catalyst for visible light region. There are several types of morphological modifications previously reported such as nanorod, nonocubes, nanospheres and flower-like [9]. To the best of our knowledge, synthesis of fibrous silica titania (FST) was conducted in this study for photodegradation of MB. The catalysts were characterized by FESEM, UV-vis/DRS, FTIR and N_2 adsorption–desorption. The synthesized FST catalyst has a unique morphology, narrow band gap, high surface area, more interaction of Si-O-Ti that acts as an active site for improving electron-hole separation and high stability that can enhance the photocatalytic performance in visible light.

2. Materials and Methods

2.1. Materials

Cetyltrimethylammonium bromide (CTAB, 99%) and methylene blue (MB, 100%) were purchased from Merck Sdn. Bhd., Malaysia. Urea (99.5%) and toluene (99.5%) were purchased from QRec, Malaysia. 1-Butanol (99.5%) and tetraethyl orthosilicate (TEOS, 95%) were purchased from Sigma Aldrich and Acros Organics, Malaysia respectively. Commercial TiO_2 powder catalyst (JRC-TiO_2) was supplied by the Catalysis Society of Japan. All chemicals were of analytical grade and used without any treatment.

2.2. Catalyst preparation

FST was synthesized by using hydrothermal method which had been established in previous study with some modification using TiO_2 seed (JRC TiO_2-2) [11]. 25 g of CTAB and 14 g of urea were diluted in distilled water and stirred for 5 minutes. 6 g of titania seed, 600 mL of toluene and 30 mL of 1-butanol were added into the solution. After that, 56 mL of TEOS was then added into the solution and stirred for 2 hours. After 2 hours, the resulting solution was kept in microwave for 6 hours at 120^{o}C. The product was left to dry overnight at 110^{o}C before calcined at 550^{o}C for 3 hours.

2.3. Characterization

The physicochemical properties of the synthesized FST were characterized using several instruments. The morphological of the catalyst were analysed by FESEM (JEOL JFC-1600, Japan). The

interactions existed in the catalysts were analyzed by FTIR spectroscopy (Perkin Elmer Spectrum GX FTIR Spectrometer, U.S). IR absorbance data with wavenumbers ranging from 400 to 4000 cm^{-1} was obtained. The wavelength of the catalysts was measured using UV-Vis/DRS which recorded over a range of wavelengths from 200 to 800 nm using a Perkin-Elmer Spectrophotometer and the band gap was calculated by equation below as shown below. The band gap was also obtained by plotting kulbelka munk.

$$Band\ gap\ (eV) = \frac{1240}{Wavelength} \quad (1)$$

2.4 Photocatalytic testing

The photoactivity of the catalyst was tested via photodegradation of MB. An amount of photocatalyst was dispersed into 250 mL of MB with a desired concentration and pH. The solution was stirred in a dark for 1 hours and then exposed under visible light for another 2 hours. During the process, 1.5 mL of MB solution sample was collected every 15 minutes and centrifuged using Beckman Coulter Microfuge at 14,000 rpm for 10 minutes. Then, the concentration of MB centrifuged liquid was examined by UV-Vis spectrophotometer (Cary 60 UV-vis Agilent, U.S) at the absorption band of 664 nm. The experiment was conducted under different parameter such as catalyst dosage (0.1-0.5 g L^{-1}), MB initial concentration (10-100 mg L^{-1}), pH (3-9) and. While, kinetic study was analysed based on the performance for different initial concentration. The efficiency of photocatalytic degradation was calculated by equation below.

$$Degradation\ (\%) = \frac{C_O - C_t}{C_O} \times 100 \quad (2)$$

3. Results and Discussion

3.1 Morphological studies of FST

The morphological properties of FST catalyst was investigated by field emission scanning electron microscopy (FESEM) as shown in figure 1A and B at magnification 50,000 X and 10,000 X, respectively. In Fig. 1A, it was obvious that a clear spherical shape with dendrimeric fibre was formed, signifying that the FST with fibrous morphology was successfully synthesized by hydrothermal method. Meanwhile, figure 1B illustrates the particle size of FST ranging from 0.46 to 0.77 µm. Similar phenomenon has been reported in previous study where the fibrous silica ZSM5 showed a well-defined uniform spherical structure with cockscomb-like surface and high porosity [12]. This morphology is expected to provide more accessibility of active sites for enhancing the adsorption of pollutants and photodegradation due to its unique structure [8,12]. Besides, the morphology of TiO_2 anatase showed low surface area with agglomeration as reported in previous study [13]. Hence, the unique morphology of FST would also enhance the performance compared to TiO_2.

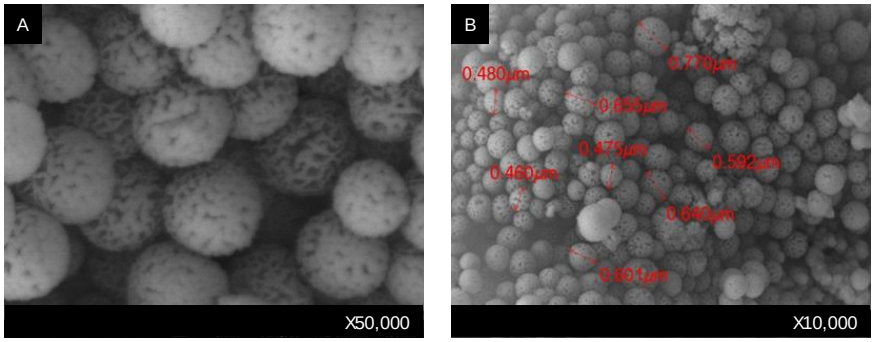

Figure 1. FESEM images of FST catalyst at magnification A) 50,000X and B)10,000X.

3.2 Vibrational spectroscopy analysis

Figure 2 illustrates the FTIR spectra of the FST, SiO_2 and commercial TiO_2 to verify the functional groups present in catalysts. It was observed that all catalysts have two bands at 3452 cm^{-1} and 1630 cm^{-1}, which attributed to a stretching and bending vibrations of adsorbed water molecules, respectively [14]. Synthesized FST resulted in increasing intensity for these bands, which indicates that the introduction of TiO_2 on fibrous silica (FS) has made the catalyst to possess more surface hydroxyl groups. The hydroxyl groups play an important role in the photocatalytic reaction since they can capture photoinduced holes and form hydroxyl radicals with high oxidation capability [15]. The bands at 1088, 796 and 468 cm^{-1} were ascribed to asymmetric and symmetric stretching, and bending vibrations of Si-O-Si, respectively [14]. Compared to the commercial TiO_2 and FS spectra, it was clearly observed that the intensity for FST at these bands were increasing. This trend indicated a major arrangement of silica framework during synthesis [16].

The bands in the range of 900-1000 cm^{-1} illustrated the significant region usually involved in the rearrangement of SiO_2 framework subsequent to modification [17]. Previous study has reported that the band existed in this range was assigned to Si-O-H stretching, non-bridging free broken Si-O stretching and Si-O-Ti bonds [18]. In this study, the band at 966 cm^{-1} was increased for FST showing that silica framework had been embedded by titania. The existence of a band at 680 cm^{-1} was observed for commercial TiO_2 and FST which corresponded to Ti-O-Ti bands signifying the presence of TiO_2 in the catalyst [19]. However, this band was seen reducing for FST, which might be due to the formation of more Si-O-Ti bonds. Thus, FST has proved that the formation of Si-O-Ti which act as an active site for electron hole separation can enhance the degradation performance.

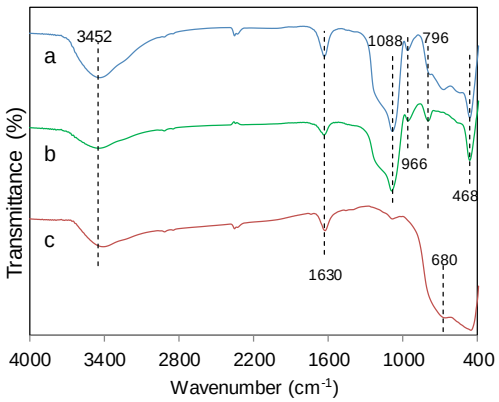

Figure 2. FTIR spectra of catalysts (a) FST, (b) Fibrous silica and (c) commercial TiO_2 at region 400-4000 cm^{-1}.

3.3 Band gap analysis

The UV–vis DRS spectra of FST and TiO_2 are illustrated in figure 3A. It can be seen that the wavelength of FST was shifted to above 400 nm compared to TiO_2 which was below 400 nm, demonstrating a significant improvement of the catalysts towards visible light absorption [17]. Kubelka-Munk plot was used to estimate the band gap energy of the prepared samples as shown in figure 3B. The band gaps were optically obtained as presented in table 1. It was observed that the band gap of FST (2.92 eV) was lower than commercial TiO_2 (3.19 eV), which attributed to easy generation of electrons and holes of FST under visible light irradiation and resulted in higher photocatalytic activity. It has been previously reported that the wide band gap above 3.0 eV contributes to high recombination rate of the photo-induced electrons and holes, which then limits the photocatalytic activity [20]. Hence, it is believed that the FST could result in a better performance in visible light. Table 1 lists the surface area of FST and TiO_2. The synthesized FST showed increasing surface area compared to TiO_2. This would lead to high accessibility of active sites and hence improved the catalytic performance [8].

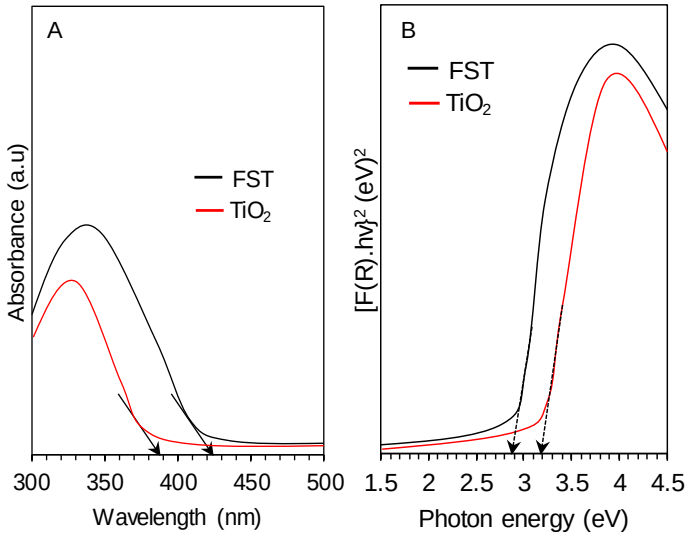

Figure 3. Kulbelka munk plot of the FST and TiO_2.

Table 1. Band gap and surface area analysis.

[a]

Catalysts	Surface area, S_{BET} (m^2 g^{-1})[a]	Pore volume, V (cm^3 g^{-1})[b]	Average pore size (nm)[b]	Band gap (eV)[c]
Commercial TiO_2	20	0.1	32.6	3.19
FST	616	1.54	45.7	2.92

Calculated from N_2 adsorption measurements using BET method

[b] Calculated from N_2 adsorption measurements using t-plot method

[c] Calculated band gap using kulbelka-munk

3.4 Photocatalytic performance and kinetic study

The photocatalytic performance of FST was studied with respect to the photodegradation of MB and compared with TiO_2 commercial as illustrated in figure 4. It was clearly showed that when the reaction was performed in the dark for 1 hour, the adsorption capacity of FST became much higher than commercial TiO_2. This was probably due to the adsorption property of silica-supported TiO_2, which might further influence the photodegradation of MB [21]. After adsorption step, the reactions continued in visible light for another 2 hours. The photodegradation rate of MB was seen to favour FST compared to commercial TiO_2 with 99.9% and 94.6%, respectively. At 60 minutes, almost all of the MB was degraded by FST catalyst while the commercial TiO_2 required more than 120 minutes. This was due to the superior properties of FST including unique morphology, narrow band gap, high surface area and more Si-O-Ti interaction.

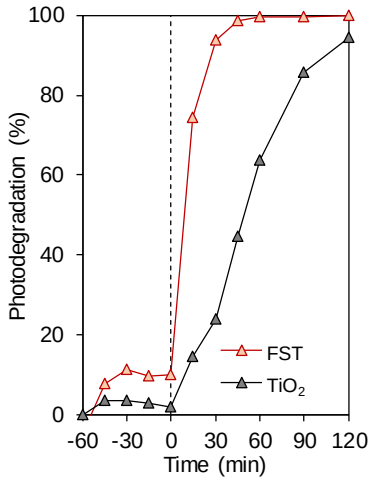

Figure 4. Photodegradation of MB using FST and TiO_2 [pH=5, W=0.25 g L^{-1}, initial concentration =10 mg L^{-1}, t=2 h].

The effects of pH were investigated ranging from of 3-9 in the presence of the FST catalyst with the results shown in figure 5A. It was seen that under various pH, the best performance was at pH 5, indicating that the reaction was favoured in a slightly acidic condition. Fig. 5B shows the effects of catalyst dosage towards photodegradation of MB at pH 5 using 10 mg L^{-1} of MB solution. The catalyst dosage was varied from 0 to 0.5 g L^{-1}. It was noticed that the photodegradation percentage of MB as the catalyst dosage increases. This might be due to the increase in active site by increasing the catalyst dosage, thus enhancing the catalytic reaction [17]. Although the overall performance was similar in the range of 0.125-0.5 g L^{-1}, the best performance was attained by 0.25 g L^{-1} of FST dosage with 99.9% under visible light compared to others, which is more favourable in adsorption process. Meanwhile, further increase in catalyst dosage resulted in a decrease of photodegradation of MB due to the increase in catalyst dosage that induced the turbidity of the system, causing light scattering and hindered the light penetration as well as triggered agglomeration of the catalyst that inhibited the photodegradation process [18]. The excess amount of catalyst dosage might lead to a decreasing production of electron-hole pairs due to inhibition of light penetration, thus producing fewer hydroxyl radicals and making the reaction rate decreased.

The photodegradation of MB at different initial concentrations ranging from 10 to 100 mg L^{-1} using 0.25 g L^{-1} of FST dosage at pH 5 is shown in figure 5C. The result clearly showed that the photodegradation percentage for 10, 25, 40, 55, 70, 85 and 100 mg L^{-1} were 99.9%, 97.9%, 87.8%, 80.7%, 73.6%, 58.5% and 47.6%, respectively. Based on the results, it can be seen that the increase in initial concentration of MB led to the decrease in performance. As the initial concentration of MB increases, more dye molecules were adsorbed on the surface of FST, which resulted in lack of direct

contact with the holes or hydroxyl radicals making inhibitive effect of dye degradation [22]. The performance of the catalyst at 10 mg L^{-1} was the highest which was 99.9% possibly due to the less adsorption of dye molecules on the catalyst surface. Hence, more photons could penetrate in the catalyst due to more accessible of light.

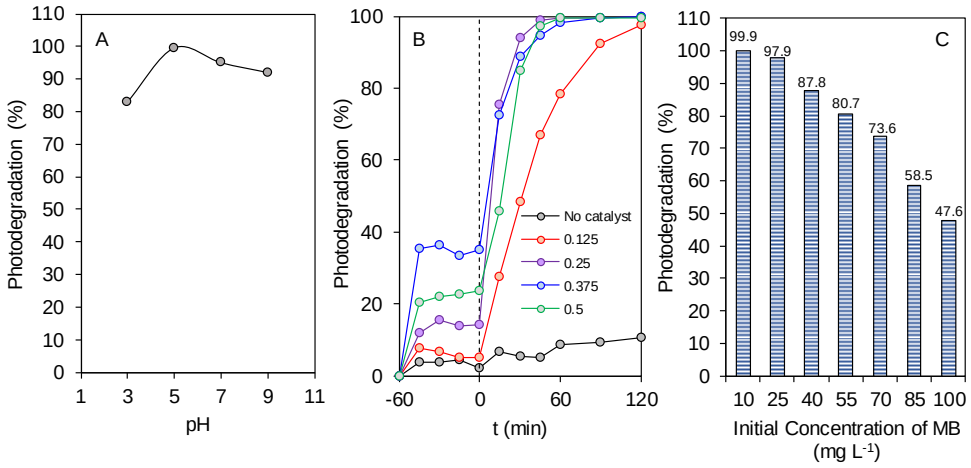

Figure 5. Photodegradation of MB (A) Effect of catalyst dosage [Co = 10 mg L^{-1}; pH = 5; t = 2 h], (B) Effect of initial concentration [pH = 5; W = 0.25 g L^{-1}; t = 2 h].

Based on the initial concentration, the photodegradation kinetics of MB was also studied. A linear fitting of $\ln(C_o/C_t)$ versus irradiation time (t) was plotted in figure 6A and the data was summarized in table 2. The results demonstrated that 10 mg L^{-1} gave the highest photodegradation rate among others concentrations. Lower photodegradation rate was shown by increasing concentrations than 10 mg L^{-1} due to the existence of large amount of adsorbed dye molecules result in lack of direct contact between the catalyst and the holes or hydroxyl radical.

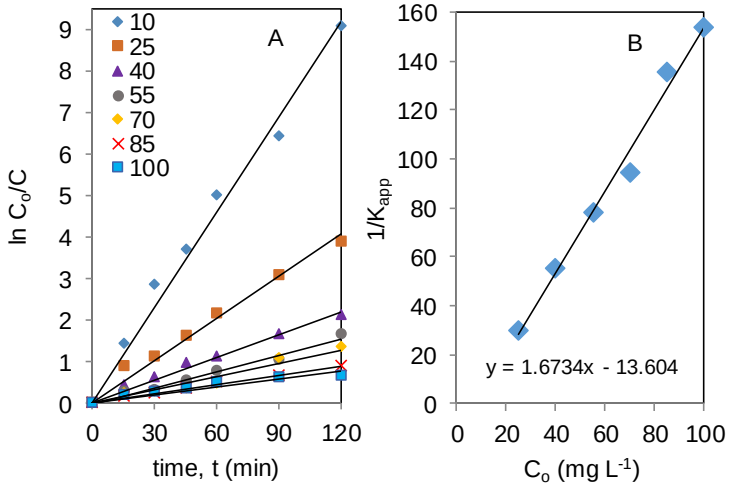

Figure 6. (A) Kinetics study (B) Relationship between 1/Kapp and Co of photodegradation of MB.

Table 2. The kinetics parameter of photodegradation using FST.

Initial concentration (mg L^{-1})	Reaction rate constant, k (min^{-1})
10	0.0766
25	0.0339
40	0.0182
55	0.0128
70	0.0098
85	0.0074
100	0.0065

Predominantly, for most of the organic compound, the effect of the photocatalytic degradation was outlined by pseudo-first-order kinetic model of Langmuir-Hinshelwood (L-H) model [19]. The L-H model is commonly used to interpret the kinetic data due to the limitation of mass transfer that occurs on the catalyst surface. At low concentration of MB, the general equation of the rate of photodegradation is given by equation 3.

$$\ln\left(\frac{C_o}{C_t}\right) = k_r\, K_{LH} = K_{app}\, t \tag{3}$$

The straight line plotted on a graph in figure 6A confirmed that photocatalytic degradation of MB follows the pseudo-first-order kinetic model. The slope of each line represents the apparent first-order rate constant [23]. Based on the L-H model, a linear plot was obtained by plotting 1/kapp as a function of C_o in figure 6B.

$$\frac{1}{K_{app}} = \left(\frac{1}{k_r}\right) C_O + \frac{1}{k_r\, K_{LH}} \tag{4}$$

Referring to Fig. 6B, the slope of the graph and the y-intercept were 1.6734 and -13.604 respectively. By simplifying the data obtained with equation 4, the reaction rate constant (k_r) and the adsorption equilibrium constant (K_{LH}) were calculated and the resulted values were 0.5976 mg L^{-1} min^{-1} and 0.123 L mg^{-1} respectively. The value of k_r was larger than K_{LH} which signified that the reaction would occur at the surface of the catalyst and it represents the rate determining step in the photocatalytic process [24,25].

3.5 Stability test

The durability of catalyst in wastewater treatment is also a plays an crucial role in order to reduce the operational cost [26]. Hence, the stability of FST for photodegradation of MB was conducted by repeating the reaction. As shown in figure 7, the FST possess high stability stable with only a slightly deactivation even after five successive recycles for the degradation. This was due to the heat treatment, which caused agglomeration of the catalysts which led to decrease of surface areas [27].

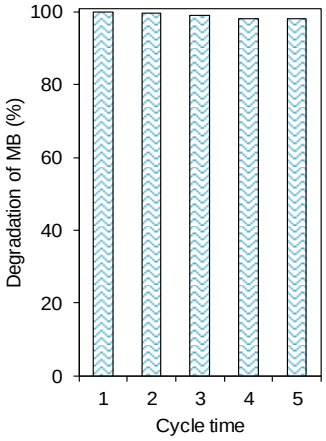

Figure 7. Stability test of FST for photodegradation of MB.

4. Conclusions

As a conclusion, FST was successfully synthesized via hydrothermal method and characterized by field emission scanning electron microscopy (FESEM), fourier transform infrared (FTIR), UV-vis diffuse reflectance spectroscopy (UV-vis/DRS) and N_2 adsorption-desorption. The potential of the synthesized FST and commercial TiO_2 were evaluated towards photocatalytic degradation of MB under visible light for 2 hours. The conditions were varied during reaction such as pH, catalyst dosage and initial concentration. It was proven that FST exhibited higher photodegradation percentage of MB than commercial TiO_2 which were 99.9% and 94.6% respectively. This was due to the unique morphology, narrow band gap, existing of interaction of Si-O-Ti that acts as an active site and large surface area obtained by FST. This study had proved that the most effective parameters for photocatalytic degradation of MB were 0.25 g L^{-1} of catalyst dosage, 10 mg L^{-1} of initial concentration and pH 5 for 2 hours of irradiation time. Based on the Langmuir-Hinshelwood model, k_r showed larger value than K_{LH}, which suggests that the reaction between OH radicals and dye molecules over the catalyst surface represents the rate determining step in photocatalytic process.

Acknowledgments

The work was supported by Fundamental Research Grant No. FRGS/1/2017/STG07/UTM/01/1 (Grant No. 4F969)

References

[1] Elmoubarki R, Mahjoubi F Z, Tounsadi H, Moustadraf J, Abdennouri M, Zouhri A, El Albani A and Barka N 2015 *Water Resour. Ind.* **9** 16-29

[2] El-Yazeed W S A and Ahmed A I 2019 *Inorg. Chem. Commun.* **105** 102-111

[3] Khalil M, Anggraeni E S, Ivandini T A and Budianto E 2019 *Appl. Surf. Sci.* **487** 1376-1384

[4] Mustapha F H, Jalil A A, Mohamed M, Triwahyono S, Hassan N S, Khusnun N F, Hitam C N C, Rahman A F A, Firmanshah L and Zolkifli A S 2017 *J. Clean Prod.* **168** 1150-1162

[5] Chong M N, Jin B, Chow C W and Saint C 2010 *Water Res.* **44** 2997-3027

[6] Fauzi A A, Jalil A A, Mohamed M, Triwahyono S, Jusoh N W C, Rahman A F A, Aziz F F A, Hassan N S, Khusnun N F and Tanaka H, J 2018 *Environ. Econ. Manag.* **227** 34-43

[7] Nguyen C H, Fu C C and Juang R S 2018 *J. Clean Prod.* **202** 413-427

[8] Singh R, Bapat R, Qin L, Feng H and Polshettiwar V 2016 *Catalysis* **6** 2770-2784

[9] Ke X, Xu L, Zeng C, Zhang L and Xu N 2007 *Micropor. Mesopor. Mater.* **106** 68-75

[10] Polshettiwar V, Cha D, Zhang X and Basset J M 2010 *Angew. Chem. Int. Ed.* **49** 9652–9656

[11] Firmansyah M L, Jalil A A, Triwahyono S, Hamdan H, Salleh M M, Ahmad W F W and Kadja G T M 2016 *Catal. Sci. Tech.* **6** 5178

[12] Aziz F F A, Jalil A A, Triwahyono S and Mohamed M 2018 *Appl. Surf. Sci.* **445** 84-95

[13] Nasikhudin, Diantoro M, Kusumaatmaja A and Triyana K 2018 *Journal of Physics: Conf. Series*. **1011** 012069

[14] Karim A, Jalil A, Triwahyono S, Sidik S, Kamarudin N, Jusoh R, Jusoh N and Hameed B J 2012 *Colloid Interface Sci.* **386** 307-314

[15] Huo Y D, Wang X C, Wu L, Chen X F, Ding Z X, Wang X X and Fu X Z 2008 *Chemosphere.* **72** 414-421

[16] Rahman A F A, Jalil A A, Triwahyono S, Ripin A, Aziz F F A, Fatah N A A, Jaafar N F, Hitam C N C, Salleh N F M and Hassan N S 2017 *J. Clean Prod.* **143** 948-959

[17] Hitam C N C, Jalil A A, Triwahyono S, Ahmad A, Jaafar N F, Salamun N, Fatah N A A, Teh L P, Khusnun N F and Ghazali Z 2016 *RSC Adv.* **6** 76859

[18] Vasconcelos D C L, Nunes E H M, Gasparon M and Vasconcelos W L 2011 *Mater. Sci. App.* **2** 1375

[19] Ansari S A and Cho M H 2016 *Sci. Rep.* **6**

[20] Kim H J, Shul Y G and Han H 2005 *Top Catal.* **35** 287-293

[21] Xu C, Rangaiah G and Zhao X 2014 *Ind. Eng. Chem. Res.* **53** 14641-14649

[22] Ranjbar P Z, Ayati B and Ganjidoust H 2019 *J. Environ. Sci.* **79** 213-224

[23] Yang L Y, Dong S Y, Sun J H, Feng J L, Wu Q H and Sun S P 2010 *J. Hazard Mater.* **179** 438-443

[24] Adam F, Muniandy L and Thankappan R 2013 *J. Colloid Interface Sci.* **406**, 209-216

[25] Hassan N S, Jalil A A, Triwahyono S, Hitam C N C, Rahman A F A, Khusnun N F, Mamat C R, Asmadi M, Mohamed M, Ali M W and Prasetyoko D 2018 *J. Taiwan Inst. Chem. Eng.* **82** 322-330

[26] Zhang S, Chen X and Song L 2019 *J. Hazard. mater.* **367** 304-315

[27] Abderrahmane H, Luc B, Pascal R, Ahmed A, Hatem E, Rabah B and Yannick C 2016 *Mater. Des.* **109** 634-643